

Synthesis and Structural Characterization of the First Quaternary Plutonium Thiophosphates: $K_3Pu(PS_4)_2$ and $APuP_2S_7$ ($A = K, Rb, Cs$)

Ryan F. Hess,[†] Pamela L. Gordon,[‡] C. Drew Tait,[‡] Kent D. Abney,[§] and Peter K. Dorhout^{*†}

Contribution from the Department of Chemistry, Colorado State University, Fort Collins, Colorado 80523, Isotope and Nuclear Chemistry (C-INC), Chemistry Division, Los Alamos National Laboratory, Los Alamos, New Mexico 87545, and Structural Inorganic Chemistry (C-SIC), Chemistry Division, Los Alamos National Laboratory, Los Alamos, New Mexico 87545

Received March 28, 2001. Revised Manuscript Received November 2, 2001

Abstract: The first quaternary plutonium metal thiophosphates have been synthesized by the reactive flux method and characterized by single-crystal X-ray diffraction: $K_3Pu(PS_4)_2$ (**I**), $KPuP_2S_7$ (**II**), $RbPuP_2S_7$ (**III**), and $CsPuP_2S_7$ (**IV**). All four compounds crystallize in the monoclinic space group $P2_1/c$ with $Z = 4$. Compound **I** has cell parameters of $a = 9.157(1)$ Å, $b = 16.866(2)$ Å, $c = 9.538(1)$, and $\beta = 90.610(3)^\circ$. Compound **II** has cell parameters of $a = 9.641(1)$ Å, $b = 12.255(1)$ Å, $c = 9.015(1)$ Å, and $\beta = 90.218(1)^\circ$. Compound **III** has cell parameters of $a = 9.8011(6)$ Å, $b = 12.3977(7)$ Å, $c = 9.0263(5)$ Å, and $\beta = 90.564(1)^\circ$. Compound **IV** has cell parameters of $a = 10.1034(7)$ Å, $b = 12.5412(9)$ Å, $c = 9.0306(6)$ Å, and $\beta = 91.007(1)^\circ$. Compound **I** is isostructural to a family of rare-earth metal thiophosphates and comprises bicapped trigonal prismatic PuS_8 polyhedra linked in chains through edge-sharing interactions and through thiophosphate tetrahedra. Compounds **II–IV** crystallize in a known structure type not related to any previously observed actinide thiophosphates and contain the $(P_2S_7)^{4-}$ corner-shared bitetrahedral ligand as a structural building block. A summary of important bond distances and angles for these new plutonium thiophosphate materials is compared to the limited literature on plutonium solid-state compounds. Diffuse reflectance spectra confirm the Pu(III) oxidation state and Raman spectroscopy confirms the tetrahedral PS_4^{3-} building block in all structures.

Introduction

The fundamental chemistry of plutonium has been summarized in several sources.^{1–3} Aside from the extensive work in metal oxide chemistry and metallurgy, many of the fundamental bonding characteristics, coordination geometries, and solid-state chemical properties of other compositions of this unusual metal have been overlooked due to the hazards associated with its inherent radioactivity. Nevertheless, the extreme stability at high temperatures (mp = 2350 °C) and its relative inert behavior toward steam at 250 °C makes PuS an attractive candidate for fast reactor nuclear fuel, possessing chemical stability that exceeds that of nitrides and phosphides.⁴ Because of the importance of stockpiles of plutonium to the world energy stores, there still remains a need for the study of fundamental solid-state chemistry of more complex plutonium sulfides.

We have made extensive explorations into the quaternary phase space of rare-earth metal chalcophosphate systems and investigated many of the bonding characteristics and coordination geometries of the 4f-elements, and recently the 5f-elements, with the softer members of the chalcogen family.^{5–9} As a complement to this work, we have initiated studies into the transuranic series of metal chalcogens in an attempt to better understand the fundamental solid-state chemistry of plutonium in chalcogen-rich environments.

Our initial work on plutonium, reported here, expands the use of the reactive chalcophosphate flux.^{10,11} The use of these reactive, moderate-temperature molten alkali-metal chalcophosphate fluxes has yielded families of complex, quaternary f-element thiophosphate compounds.^{5,9,12–15} Recently, this

* To whom correspondence should be addressed. Telephone: (970) 491-0624. E-mail: pkd@lamar.colostate.edu.

[†] Colorado State University.

[‡] Structural Inorganic Chemistry, Los Alamos National Laboratory.

[§] Isotope and Nuclear Chemistry, Los Alamos National Laboratory.

(1) Weigel, R.; Katz, J. J.; Seaborg, G. T. In *The Chemistry of the Actinide Elements*; Katz, J. J., Seaborg, G. T., Morss, L. R., Eds.; Chapman and Hall: New York, 1986; Vol. 1, pp 499–886.

(2) *Plutonium Handbook*; American Nuclear Society: LaGrange Park, IL, 1980.

(3) Cleveland, J. M. *The Chemistry of Plutonium*; American Nuclear Society: LaGrange Park, IL, 1979.

(4) Allbutt, M.; Dell, R. M. *J. Nucl. Mater.* **1967**, *24*, 1–20.

(5) Evenson, C. R.; Dorhout, P. K. *Inorg. Chem.* **2001**, *40*, 2884–2891.

(6) Evenson, C. R.; Dorhout, P. K. *Inorg. Chem.* **2001**, *40*, 2875–2883.

(7) Briggs Piccoli, P. M.; Abney, K. D.; Schoonover, J. R.; Dorhout, P. K. *Inorg. Chem.* **2000**, *39*, 2970–2976.

(8) Briggs-Piccoli, P. M.; Abney, K. D.; Schoonover, J. R.; Dorhout, P. K. *Inorg. Chem.* **2001**, *40*, 4871–4875.

(9) Hess, R. F.; Abney, K. D.; Burris, J. L.; Hochheimer, H. D.; Dorhout, P. K. *Inorg. Chem.* **2001**, *40*, 2851–2859.

(10) Sunshine, S. A.; Kang, D.; Ibers, J. A. *J. Am. Chem. Soc.* **1987**, *109*, 6202–6204.

(11) Kanatzidis, M. G. *Curr. Opin. Solid State Mater. Sci.* **1997**, *2*, 139–149.

(12) Gauthier, G.; Jobic, S.; Brec, R.; Rouxel, J. *Inorg. Chem.* **1998**, *37*, 2332–2333.

chemistry has been extended to include thorium and uranium.⁹ These 5f-element compounds have structures ranging from three-dimensional networks as in $\text{Cs}_8\text{U}_5(\text{P}_3\text{S}_{10})_2(\text{PS}_4)_6$, to isolated dimeric clusters found in the series $\text{A}_5\text{An}(\text{PS}_4)_3$ ($\text{A} = \text{K}, \text{Rb}, \text{Cs}$; $\text{An} = \text{Th}, \text{U}$). All of the thiophosphate actinide chemistry studied so far has focused on either thorium or uranium. Our original hypothesis for plutonium chemistry in the complex melts of alkali-metal chalcophosphate melts is that this actinide metal chemistry will behave more like a rare-earth metal than an earlier actinide metal.

The use of moderate-temperature reactive molten salts is the key to the synthetic paradox that has limited plutonium solid-state chemistry. The low melting point of plutonium (640 °C) and the vigorous reactivity of the liquid with most conventional reaction vessels prevent a safe exploration of any moderate-to-high temperature synthetic chemistry.^{2,3} As has been shown for transition metal and lanthanide metal chemistry, the thiophosphate flux can facilitate the low-to-moderate temperature reactions of metals with the flux components while promoting the nucleation and growth of single-crystalline products. We report the synthesis and characterization of the first plutonium thiophosphate compounds $\text{K}_3\text{Pu}(\text{PS}_4)_2$ (**I**) and APuP_2S_7 (**II**, **III**, **IV**), where $\text{A} = \text{K}, \text{Rb}, \text{Cs}$. Compound **I** is isostructural with $\text{K}_3\text{Ce}(\text{PS}_4)_2$ synthesized by Brec and co-workers and our $\text{K}_3\text{La}(\text{PS}_4)_2$ and has an isolated, infinite chain structure.^{6,12} The structure of compounds **II–IV** is related to KBiP_2S_7 ¹⁶ and the recently reported KSmp_2S_7 ,¹⁵ and comprises layers of Pu atoms linked by $(\text{P}_2\text{S}_7)^{4-}$ ligands, a structural building unit that has not been seen in any of our corresponding actinide work.

Experimental Section

General Synthesis. Red phosphorus powder (99.9%) was obtained from Cerac. Sulfur powder (99.999%) was purchased from Johnson Matthey. ²³⁹Pu shot was obtained from Los Alamos National Laboratory purified from impure metal by electrorefining in a NaCl/KCl eutectic. K_2S_3 , Rb_2S_5 , and Cs_2S_2 were prepared from the reaction of stoichiometric amounts of the elements in liquid ammonia as described elsewhere.^{17,18} Ampules for the reactions were fused-silica tubes with 4 mm inner diameter and a 6 mm outer diameter. All reagents were stored and manipulated in an argon-filled negative pressure specialty glovebox.

Warning: ²³⁹Pu is a radioactive element with a half-life of 2.41 × 10⁴ years—extreme caution must be used to prevent inhalation or ingestion.

Synthesis of $\text{K}_3\text{Pu}(\text{PS}_4)_2$ (I**).** $\text{K}_3\text{Pu}(\text{PS}_4)_2$ was synthesized from a mixture of 0.1150 g (0.481 mmol) of Pu, 0.0298 g (0.962 mmol) of P, 0.1619 g (5.05 mmol) of S, and 0.1259 g (0.723 mmol) of K_2S_3 . The mixture was loaded into a fused silica ampule and sealed under vacuum. The ampule was then heated to 500 °C over 16 h and held there for 200 h. The ampule was cooled to ambient temperature at a rate of 3 °C per hour. The ampules were opened in an inert atmosphere glovebox, and the products were removed from the container. Excess flux was removed by washing with DMF. Emerald green plates were then isolated by filtration and selected crystals were handpicked for analysis. No unreacted Pu metal was evident.

Table 1. Crystallographic Data for **I–IV**

| | I | II | III | IV |
|--|------------------------------------|---------------------------|----------------------------|----------------------------|
| empirical formula | $\text{K}_3\text{PuP}_2\text{S}_8$ | KPuP_2S_8 | RbPuP_2S_7 | CsPuP_2S_7 |
| fw | 677.72 | 567.46 | 613.83 | 661.27 |
| <i>a</i> , Å | 9.157(1) | 9.641(1) | 9.8011(6) | 10.1034(7) |
| <i>b</i> , Å | 16.866(2) | 12.255(1) | 12.3977(7) | 12.5412(9) |
| <i>c</i> , Å | 9.538(1) | 9.0152(8) | 9.0263(5) | 9.0306(6) |
| β , deg | 90.610(3) | 90.218(2) | 90.564(1) | 91.007(1) |
| <i>V</i> , Å ³ | 1473.0(3) | 1065.1(2) | 1096.7(1) | 1144.1(1) |
| <i>Z</i> | 4 | 4 | 4 | 4 |
| λ (Mo K α), Å | 0.71073 | 0.71073 | 0.71073 | 0.71073 |
| space group | $P2_1/c$ (No.14) | $P2_1/c$ (No.14) | $P2_1/c$ (No.14) | $P2_1/c$ (No.14) |
| temp, K | 163(2) | 163(2) | 163(2) | 163(2) |
| ρ_{calc} , g/cm ³ | 3.056 | 3.539 | 3.718 | 3.839 |
| μ , mm ⁻¹ | 6.63 | 8.18 | 11.98 | 10.39 |
| R1, ^a % | 0.0371 | 0.0324 | 0.0510 | 0.0486 |
| wR2, ^a % | 0.0918 | 0.0689 | 0.1455 | 0.1221 |

$$^a \text{R1} = \sum(|F_o| - |F_c|)/\sum|F_o|; \text{wR2} = [\sum(w(F_o^2 - F_c^2)^2)/\sum(w(F_o^2)^2)]^{1/2}.$$

Synthesis of APuP_2S_7 (II–IV**).** KPuP_2S_7 (**II**) was synthesized from a mixture of 0.0930 g (0.389 mmol) of Pu, 0.072 31 g (2.34 mmol) of P, 0.1497 g (4.67 mmol) of S, and 0.083 06 g (0.584 mmol) of K_2S_3 . For RbPuP_2S_7 (**III**), a mixture of 0.0550 g (0.230 mmol) of Pu, 0.0279 g (0.921 mmol) of P, 0.0554 g (1.727 mmol) of S, and 0.114 g (0.345 mmol) of Rb_2S_5 was used. For CsPuP_2S_7 (**IV**), a mixture of 0.0660 g (0.276 mmol) of Pu, 0.034 14 g (1.10 mmol) of P, 0.1062 g (3.31 mmol) of S, and 0.1367 g (0.414 mmol) of Cs_2S_2 was used. The mixtures were loaded into fused silica ampules and sealed under vacuum. The ampules were then heated to 500 °C over 16 h and held there for 200 h. The ampules were cooled to ambient temperature at a rate of 3 °C per hour. The ampules were opened in an inert atmosphere glovebox, and the products were removed from the container. Excess flux was removed by washing with DMF. Emerald green needles were then isolated by filtration and selected crystals were handpicked for analysis. No unreacted Pu metal was evident, and no other phases were apparent.

Structure Determination. Single-crystal X-ray diffraction was performed on a modified Siemens P4 four-circle diffractometer equipped with a SMART CCD system using graphite-monochromated Mo K α radiation.¹⁹ Crystals were selected from the reaction mixtures and placed in a pool of epoxy. The crystals were then removed from the epoxy and placed inside 0.5 mm capillary tubes. The capillary tubes were then removed from the glovebox, they were trimmed to the appropriate length, and the ends were sealed with epoxy. A coating of acrylic was applied to the surface of capillary tubes to provide the third and final layer of containment. The capillary tubes were then placed in the cold stream of the diffractometer.

Cell constants for all structures were initially calculated from reflections taken from approximately 30 frames of reflections. Final cell constants were calculated from all reflections observed in the actual data collection. Reflections were integrated using SAINT.²⁰ Table 1 summarizes the crystal structure parameters for compounds **I–IV**. For each structure, the data were processed and corrected for absorption using SADABS.²¹ The structures were solved by direct methods allowing the unambiguous space group assignments and refined in full-matrix least squares using the program SHELXTL under the XSELL package of programs.²² The final cycle of refinement included all anisotropic displacement parameters. Secondary extinction coefficients were applied to the final refinements where necessary. Additional experimental details are given in the Supporting Information as CIF files. Specific refinement issues related to each structure are explained in the Results and Discussion section.

(13) Gauthier, G.; Jobic, S.; Boucher, F.; Macaudiere, P.; Huguénin, D.; Rouxel, J.; Brec, R. *Chem. Mater.* **1998**, *10*, 2341–2347.

(14) Gauthier, G.; Jobic, S.; Danaire, V.; Brec, R.; Evain, M. *Acta Crystallogr., C* **2000**, *56*, 117.

(15) After initial submission of this paper, the structure of KSmp_2S_7 was reported in: Goh, E.-Y.; Kim, E.-J.; Kim, S.-J. *J. Solid State Chem.* **2001**, *160*, 195–204.

(16) McCarthy, T. J.; Kanatzidis, M. G. *Chem. Mater.* **1993**, *5*, 1061–1063.

(17) Schewe-Miller, I. *Metallreiche Hauptgruppenmetall-Chalkogenverbindungen: Synthese, Strukturen und Eigenschaften*. Ph.D. Thesis, Universität Stuttgart, 1990.

(18) Liao, J.-H.; Kanatzidis, M. G. *Inorg. Chem.* **1992**, *31*, 431–439.

(19) SMART-CCD; Siemens Analytical X-ray Systems, Inc.: Madison, WI, 1998.

(20) SAINT; Siemens Analytical X-ray Systems, Inc.: Madison, WI, 1996.

(21) Sheldrick, G. M. *SADABS*; University of Göttingen: Göttingen, Germany, 1997.

(22) Sheldrick, G. M. *XSELL*; Siemens Analytical X-ray Systems, Inc.: Madison, WI, 1999.

Optical and Vibrational Spectroscopy. As representative samples, only the spectra and analyses from compounds **I** and **III** are reported. Raman vibrational spectra were obtained by exciting from an Ar^+ laser (Spectra Physics, Model 2025) using the 514.5 nm line. The laser power at the sample was 10 mW or less. The scattered light was dispersed and analyzed on a SPEX Model 1403 scanning double monochromator equipped with an 1800 groove/mm grating and a single-photon-counting detection system. The spectral slit width was maintained at 5 cm^{-1} resolution. Scan parameters were 1 cm^{-1} increments between points, integration for 2–3 s at each point, and at least 75–90 scans averaged for the final spectrum. Samples were contained within a 9 mm fused silica tube fitted with a Teflon spacer. Diffuse reflectance spectra were collected using a spherical detector on a Perkin-Elmer UV–vis–NIR spectrometer. The samples for diffuse reflectance spectroscopy were prepared as a dispersion of single crystals mounted on a Teflon disk that was covered by a cylindrical glass cap sealed with epoxy.

Results and Discussion

In our thiophosphate studies carried out using Th and U, we have yet to characterize any compounds that are isostructural with any rare-earth chalcophosphates. This may be due to the difference in preferred oxidation states of the earlier 5f-metals. For both Th and U the 4+ oxidation state is by far the most common in chalcogenide chemistry and likely the most stable oxidation state, according to their redox potentials in solution.²³ Moving toward the heavier actinides, the 3+ oxidation state becomes increasingly more common and stable. In the plutonium compounds described below, we can argue that Pu(III) is likely the oxidation state based on charge balancing and spectroscopic evidence, although a compound with Pu(IV) would not be unreasonable.

A careful search of the literature reveals that only a handful of plutonium sulfide crystal structures could be found.^{1,3} These binary and ternary structures reveal four general coordination environments for plutonium (six-, seven-, eight-, and nine-coordinate Pu) with inconsistent bond distances for the plutonium–sulfur bond: 2.768 Å for PuS (reported as six-coordinate Pu(II) in a rock salt structure)²⁴ up to 3.02 Å in the Pu(III) oxysulfide, Pu_2O_2S .^{25,26} Eight-coordinate plutonium(III) (Pu–S = 2.93 Å) was found in the defect sesquisulfide, Pu_2S_3 .^{25,27} In this discussion, we will reveal a series of more consistent bond distances and coordination geometries for an environment of sulfur around plutonium(III). Finally, since compounds **II–IV** are isostructural, only the detailed description of **II** will be given here. Pertinent bond distances and angles for **III** and **IV** will be included in the discussion of the structures for the sake of comparison.

Structure Description: A. $K_3Pu(PS_4)_2$, I. The compound crystallized as emerald green plates in the monoclinic space group $P2_1/c$ ($r_{\text{int}} = 0.0182$) based on the systematic absences observed in the data. Refinement of the model's 127 parameters to the data (1726 reflections) provided an excellent goodness-of-fit (GOF = 1.065) resulting in a relatively flat electron density difference map (maximum = 1.916 e^- , minimum = -1.744

Table 2. Fractional Atomic Coordinates and Equivalent Isotropic Displacement Parameters ($\text{\AA}^2 \times 10^3$)^a for $K_3Pu(PS_4)_2$

| | <i>x</i> | <i>y</i> | <i>z</i> | <i>U</i> (eq) |
|-------|-----------|------------|-----------|---------------|
| Pu(1) | 0.7286(1) | −0.0142(1) | 0.5243(1) | 21(1) |
| P(1) | 0.0250(3) | 0.0979(2) | 0.7208(2) | 22(1) |
| P(2) | 0.4956(3) | −0.0999(2) | 0.7447(3) | 22(1) |
| K(1) | 0.7686(3) | 0.4679(2) | 0.4861(2) | 38(1) |
| K(2) | 0.3787(4) | 0.2936(2) | 0.3745(3) | 54(1) |
| K(3) | 0.8841(5) | 0.2125(2) | 0.3665(3) | 68(1) |
| S(1) | 0.8366(4) | −0.1580(2) | 0.4085(3) | 30(1) |
| S(2) | 0.8137(4) | 0.1274(2) | 0.6718(3) | 31(1) |
| S(3) | 0.0418(4) | −0.0220(2) | 0.6781(3) | 27(1) |
| S(4) | 0.4648(3) | −0.1207(2) | 0.5335(3) | 26(1) |
| S(5) | 0.7153(3) | −0.1123(2) | 0.7743(3) | 31(1) |
| S(6) | 0.4422(4) | 0.0174(2) | 0.7604(3) | 33(1) |
| S(7) | 0.3827(4) | −0.1770(2) | 0.8604(3) | 35(1) |
| S(8) | 0.0671(4) | 0.1255(2) | 0.9215(3) | 31(1) |

^a *U*(eq) is defined as one-third of the trace of the orthogonalized U_{ij} tensor.

Table 3. Bond Distances (Å) for $K_3Pu(PS_4)_2$

| | | | |
|-------------|----------|-----------|----------|
| Pu(1)–S(1) | 2.846(3) | P(1)–S(8) | 2.003(3) |
| Pu(1)–S(2) | 2.875(3) | P(1)–S(1) | 2.046(3) |
| Pu(1)–S(5) | 2.905(3) | P(1)–S(2) | 2.047(3) |
| Pu(1)–S(4A) | 2.933(3) | P(1)–S(3) | 2.068(3) |
| Pu(1)–S(3A) | 2.934(3) | P(2)–S(7) | 2.000(4) |
| Pu(1)–S(4) | 3.012(3) | P(2)–S(5) | 2.039(4) |
| Pu(1)–S(6) | 3.120(3) | P(2)–S(6) | 2.043(4) |
| Pu(1)–S(3) | 3.210(3) | P(2)–S(4) | 2.061(3) |

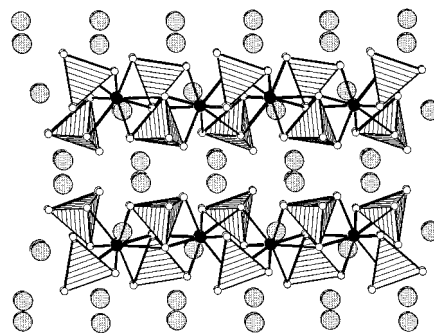


Figure 1. Polyhedral rendering of $K_3Pu(PS_4)_2$, **I**. Filled circles are Pu atoms, gray circles are K atoms, and striped polyhedra are (PS_4) units.

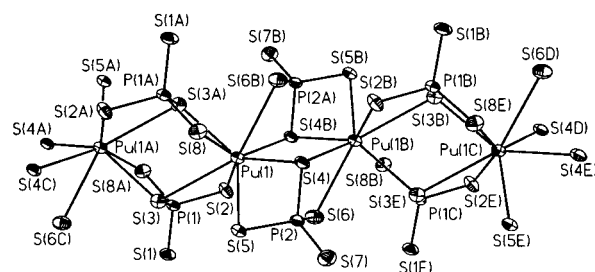


Figure 2. Thermal ellipsoid plot of $K_3Pu(PS_4)_2$, **I** (50% ellipsoids). K atoms have been removed for clarity.

e^-). Table 1 contains the specific data collection and refinement information. Tables 2 and 3 contain the atomic coordinates and relevant bond distances, respectively.

This compound comprises isolated linear chains of PuS_8 bicapped trigonal prisms linked together through both edge sharing with neighboring PuS_8 polyhedra and $(PS_4)^{3-}$ thiophosphate anions. Figure 1 shows a polyhedral packing view of the chains of plutonium(III) thiophosphate, and Figure 2 shows the coordination environment around the Pu atoms in chains running down [100]. All eight sulfur atoms bound to Pu are part of the

- (23) Bagnall, K. W. *The Actinide Elements*; Elsevier: New York, 1972; p 30. The relative redox potentials of Pu(III) versus Pu(IV) suggest that Pu(III) will likely be the most stable under thermodynamic conditions, although these oxidation states are within 1 V of each other. Np(III)/Np(IV) is +0.157 V (in acidic solutions) and suggests that higher-valent or mixed-valent neptunium chalcogenide chemistry may be possible.
- (24) Zachariasen, W. H. *Acta Crystallogr.* **1949**, *2*, 291.
- (25) Zachariasen, W. H. *Acta Crystallogr.* **1948**, *C1*, 265–268.
- (26) Zachariasen, W. H. *Acta Crystallogr.* **1949**, *2*, 60.
- (27) Zachariasen, W. H. *Acta Crystallogr.* **1949**, *2*, 57.

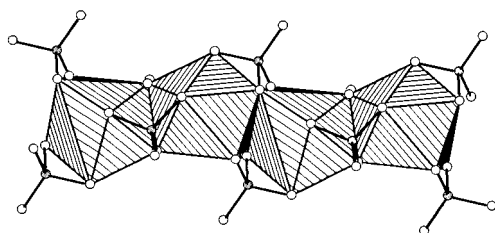


Figure 3. Polyhedral rendering of one chain in $K_3Pu(PS_4)_2$, **I**. Polyhedra are PuS_8 , gray circles are P atoms, and open circles are S atoms.

thiophosphate anions. The Pu–S bond distances range from 2.846(3) to 3.210(3) Å with an average distance of 2.979 Å. The two longest bonds in the Pu–S coordination sphere belong to the capping sulfur atoms S(3) and S(6) with distances of 3.210(3) and 3.120(3) Å respectively. In this phase, plutonium should be in the 3+ oxidation state based on charge balance and the relative Pu–S bond distances that are close to those reported for the sesquisulfide and Pu_2O_2S . The green color of the material cannot be the only indicator of plutonium oxidation state—while Pu(III) perchlorate solutions show a strong absorption between 550 and 610 nm ($\epsilon = 40 \text{ cm}^{-1} \text{ M}^{-1}$), Pu(IV) solutions will possess an equally strong absorption at 650 nm, along with an absorption at 470 nm.³ The relative redox potentials of Pu(III) and Pu(IV) in acid solutions are fairly close, and we do not know those potentials in alkali metal sulfide melts, suggesting that optical spectroscopy or magnetic analyses are needed to elucidate the true nature of the plutonium.²³ Optical data, discussed later, and recurring trends seen in other new plutonium thiophosphates reveal the true nature of the oxidation state of plutonium to be Pu(III).²⁸

Each PuS_8 polyhedron shares two of its edges (through S(3) and S(4)) with two other polyhedra to form a quasi-infinite chains of $[\infty[Pu(PS_4)_2]^{3-}]$. The two shared edges are on opposite sides of the polyhedron and are perpendicular to each other. This bonding arrangement is responsible for the chains having a kinked morphology as seen in the polyhedral rendering in Figure 3. Two distinct $(PS_4)^{3-}$ anions are present in this structure. Both anions share three of their sulfur atoms with Pu atoms. The fourth sulfur atom in both anions (S(1) and S(7)) points away from the plutonium atoms and is bound only to K^+ cations through ionic interactions. In the P(1) thiophosphate anion, S(2) and S(8) are bound to two different plutonium atoms while S(3) bridges the same two atoms. The P(2) thiophosphate anion also has one sulfur atom, S(4), that bridges two plutonium atoms and two sulfur atoms, S(5) and S(6), that are only bound to only one plutonium atom. A significant difference in the two $(PS_4)^{3-}$ anions is their orientation with respect to the chain axis. The triangular face shared by P(1) S_4 lies almost parallel to the chain axis and between two plutonium atoms, thus sharing two of its tetrahedral edges with the plutonium polyhedron. The bridging sulfur atom, S(3), has a perfect tetrahedral angle, Pu(1)–S(3)–Pu(1), of 109.50°. The tetrahedron defined as P(2) S_4 shares two edges with the plutonium polyhedra, with the bridging sulfur atom, S(4), forming a Pu(1)–S(4)–Pu(1) angle of 90.85°. The differences in the bridging angles of S(3) and S(4) and in the thiophosphate coordination lead to two

Table 4. Fractional Atomic Coordinates and Equivalent Isotropic Displacement Parameters ($\text{\AA}^2 \times 10^3$)^a for $KPuP_2S_7$

| | <i>x</i> | <i>y</i> | <i>z</i> | <i>U</i> (eq) |
|-------|-----------|-----------|------------|---------------|
| Pu(1) | 0.8563(1) | 0.6429(1) | 0.1082(1) | 11(1) |
| K(1) | 0.3929(3) | 0.6936(2) | −0.1314(3) | 25(1) |
| S(1) | 0.0163(3) | 0.4404(2) | 0.1804(3) | 14(1) |
| S(2) | 0.6621(3) | 0.5244(2) | −0.0704(3) | 16(1) |
| S(3) | 0.1492(3) | 0.6949(2) | 0.1452(3) | 14(1) |
| S(4) | 0.6270(3) | 0.5550(2) | 0.2898(3) | 17(1) |
| S(5) | 0.9095(3) | 0.8331(2) | −0.0725(3) | 14(1) |
| S(6) | 0.6254(3) | 0.7938(2) | 0.1119(3) | 16(1) |
| S(7) | 0.7502(3) | 0.0555(2) | 0.0785(3) | 14(1) |
| P(1) | 0.1867(3) | 0.5371(2) | 0.1981(3) | 12(1) |
| P(2) | 0.7226(3) | 0.8999(2) | −0.0226(3) | 11(1) |

^a *U*(eq) is defined as one-third of the trace of the orthogonalized U_{ij} tensor.

different Pu–Pu distances. In the case where two plutonium atoms are bridged by S(3) (Pu(1) and Pu(1A) in Figure 1, the Pu–Pu distance is 5.020(3) Å, whereas the two plutonium atoms bridged by S(4) display a Pu–Pu distance of 4.235(3) Å—both cases are outside the van der Waals radius of plutonium(III).

The charge-compensating K^+ cations fill the void between the plutonium thiophosphate chains; see Figure 1. K(1) and K(2) are both coordinated to eight sulfur atoms while K(3) is coordinated to seven sulfur atoms. The K–S bond distances range from 3.174(4) to 3.709(4) Å with an average distance of 3.383 Å.

The structure of $K_3Pu(PS_4)_2$ may be compared readily to the structure of $K_3La(PS_4)_2$.⁵ Both structures contain alternating short–long metal distances along one-dimensional chains. The alternating La–La distances in our $K_3La(PS_4)_2$ are 5.045(2) and 4.217(2) Å, while the Pu–Pu distances are 5.020(3) and 4.235(3) Å. In $K_3La(PS_4)_2$, the average La–S bond distances are 3.076(2) Å for a nine-coordinate La atom, and in $K_3Pu(PS_4)_2$, the average Pu–S bond distances are 2.979(3) Å for an eight-coordinate Pu atom. The difference in coordination environments of La and Pu lies in how the PS_4 tetrahedra bridge the Pu atoms along the chains. Referring to Figure 2, the P(2) thiophosphate in our $K_3Pu(PS_4)_2$ compound is twisted relative to the chain perpendicular in such a way that the S(6B)–Pu(1B) distance is 3.516(3) Å. In our $K_3La(PS_4)_2$, the thiophosphate group is twisted relative to the chain perpendicular so that the corresponding distance is 3.118(2) Å—a reasonable bonding distance to La; a concomitant shift in the S(5B) position in $K_3La(PS_4)_2$ also maintains a bonding distance to lanthanum, yielding a nine-coordinate metal ion.

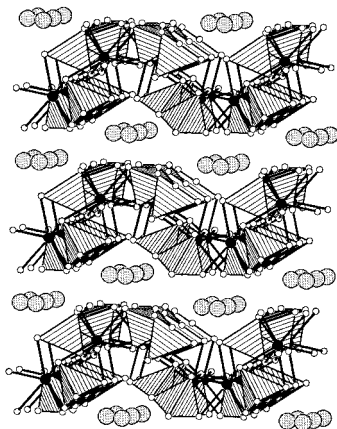
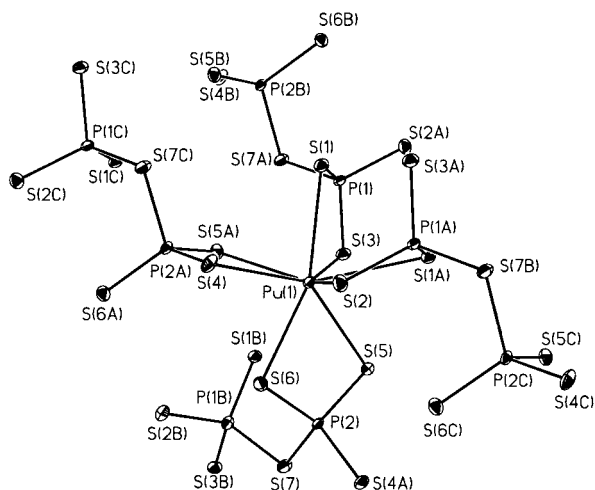
B. $KPuP_2S_7$, II. This compound crystallized as emerald green needles in the monoclinic space group $P2_1/c$ ($r_{\text{int}} = 0.0423$) based on the systematic absences in the data. Refinement of the model's 100 parameters to the data (1376 reflections) provided an excellent goodness-of-fit (GOF = 1.061) resulting in a relatively flat electron density difference map (maximum = 2.248 e^- , minimum = −0.987 e^-). Table 1 contains the specific data collection and refinement information. Tables 4 and 5 contain the atomic coordinates and relevant bond distances, respectively.

The main structural features of $KPuP_2S_7$ are the charged corrugated layers of $[\infty[PuP_2S_7]^-]$ containing one crystallographically distinct Pu atom. The corrugated nature of the layers in this structure is seen in the polyhedral representation shown in Figure 4. Such a layered structure has been observed in $KBiP_2S_7$ and $KSmP_2S_7$.^{15,16} Each Pu atom is coordinated to eight

(28) Hess, R. F.; Abney, K. D.; Dorhout, P. K. Manuscript in preparation. The structurally unrelated compound $Rb_3Pu(P_2S_6)_{1/2}(PS_4)$ was prepared and crystallized in $C2/c$ with the lattice constants $a = 22.943(2)$ Å, $b = 6.8198(3)$ Å, $c = 18.827(1)$ Å, and $\beta = 122.005^\circ$.

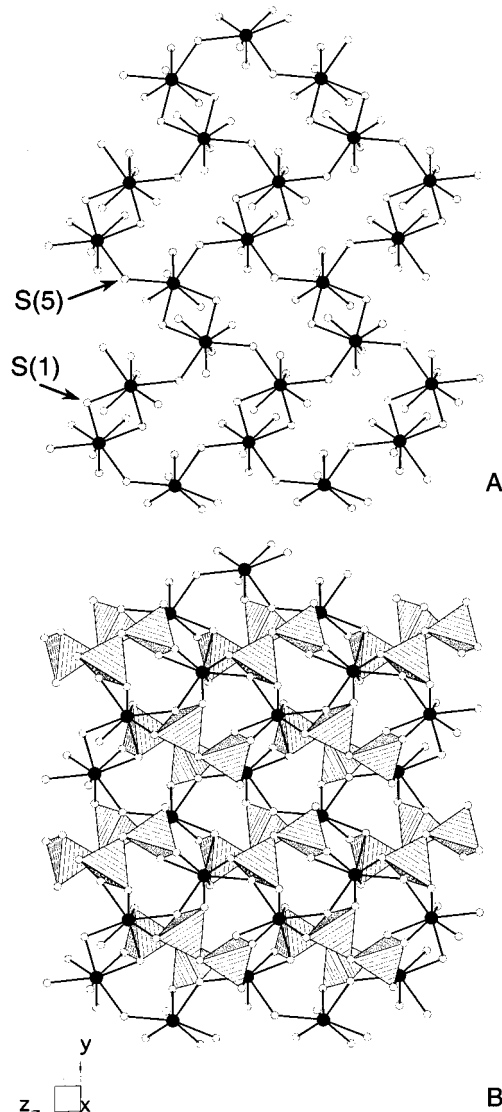
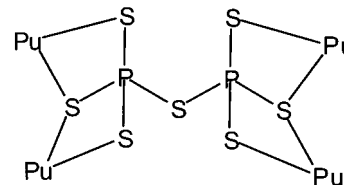
Table 5. Bond Distances (Å) for $KPuP_2S_7$

| | | | |
|-------------|----------|-----------|----------|
| Pu(1)–S(2) | 2.861(3) | P(1)–S(2) | 2.007(4) |
| Pu(1)–S(5) | 2.890(3) | P(1)–S(3) | 2.024(4) |
| Pu(1)–S(6) | 2.894(3) | P(1)–S(1) | 2.032(4) |
| Pu(1)–S(3) | 2.912(3) | P(1)–S(7) | 2.115(4) |
| Pu(1)–S(5A) | 2.937(3) | P(2)–S(4) | 2.001(4) |
| Pu(1)–S(4) | 2.960(3) | P(2)–S(6) | 2.011(4) |
| Pu(1)–S(1) | 2.993(3) | P(2)–S(5) | 2.031(4) |
| Pu(1)–S(1A) | 3.056(3) | P(2)–S(7) | 2.130(4) |

**Figure 4.** Polyhedral view of $KPuP_2S_7$, **II**, showing the corrugated nature of the layers. Filled circles are Pu atoms, gray circles are K atoms, and polyhedra are corner-sharing (PS_4) units.**Figure 5.** Thermal ellipsoid plot of $KPuP_2S_7$, **II** (50% ellipsoids), showing the environment around Pu. K atoms have been removed for clarity.

sulfur atoms in a distorted square antiprismatic geometry. Figure 5 shows the coordination environment around the Pu atom, including the $(P_2S_7)^{4-}$ ligands. This arrangement is different from that found in $KBiP_2S_7$, where bismuth is found as a seven-coordinate ion with a lone pair occupying a face-capping position on a psi-bicapped trigonal prism. The Pu–S bond distances range from 2.861(3) to 3.056(3) Å with an average distance of 2.938 Å. These distances are all consistent with those reported for the sesquisulfide and the oxisulfide, Pu_2O_2S . All eight of the coordinated sulfur atoms are belong to the $(P_2S_7)^{4-}$ thiophosphate ligand.

Unlike in the chain compound, **I**, the PuS_8 polyhedron shares only one edge with a neighboring PuS_8 polyhedron to form a dimer. Each Pu atom in the dimer corner shares one of its sulfur atoms with another PuS_8 polyhedron. Figure 6A illustrates this two-dimensional network of plutonium sulfide. In addition to

**Figure 6.** (A) View of one layer of $KPuP_2S_7$, **II**, in the bc plane with phosphorus and potassium atoms removed for clarity. Chains of corner-sharing PuS_8 run roughly along $[001]$ linked through edge-sharing PuS_8 along $[010]$. (B) The same layer as in (A), with P_2S_7 edge-sharing polyhedra. Filled circles are Pu atoms; open circles are S atoms.**Scheme 1**

the Pu–S–Pu bonding, the $(P_2S_7)^{4-}$ ligands further link the plutonium polyhedra together in a chelate fashion. The $(P_2S_7)^{4-}$ ligand comprises two PS_4 tetrahedral units that corner share one sulfur atom and has been observed in such compounds as $KBiP_2S_7$, $RbVP_2S_7$, and recently in $KSmP_2S_7$.^{15,16,29} In compounds **II–IV**, the $(P_2S_7)^{4-}$ ligand chelates four plutonium atoms in a tetradentate fashion, shown in Scheme 1. This coordination is different from that found in $KBiP_2S_7$ and in $RbVP_2S_7$. The arrangement of both edge- and corner-sharing PuS_8 polyhedra and the tetradentate $(P_2S_7)^{4-}$ ligands leads to a

(29) Durand, E.; Evain, M.; Brec, R. *J. Solid State Chem.* **1993**, *102*, 146–155.

corrugated layered structure that contains channels running perpendicular to the layers. The channels, clearly seen in Figure 6A, have the dimensions $4.29 \text{ \AA} \times 4.24 \text{ \AA}$. The layers are not offset from one another, allowing the channels to run through the entire structure perpendicular to the layers. The nine-coordinate K^+ cations lie in the interlayer spacing within the channels with interaction distances ranging from 3.232(4) to 3.887(4) \AA . The closest $\text{Pu}\cdots\text{Pu}$ interaction in this structure is 4.877 \AA , and the interlayer spacing is 3.430 \AA .

An alternate way of describing the structure in one layer is that the PuS_8 polyhedra corner share through S(5) to form chains running along the [001] direction. The polyhedra also edge share (through S(1) and S(1A)) with neighboring PuS_8 polyhedra along the [010] direction to form layers in the bc plane. Based on these corner- and edge-sharing interactions, one can see in Figure 6A that the layers contain 12-membered rings made built up of two Pu dimeric units linked together through two corner-sharing Pu polyhedra creating a 12^3 -type net.³⁰

The complete bond distance tables for RbPu_2S_7 (**III**) and CsPu_2S_7 (**IV**) can be found in the Supporting Information; however, for the sake of comparison, the Pu–S bond distances within these structures are all identical to those for **I**, within the standard deviations of the positional parameters. The layers in **III** and **IV** are propped apart slightly from **I**, a result of the longer Rb–S and Cs–S interactions (3.318(3)–3.917(4) \AA and 3.454(4)–3.965(4) \AA , respectively).

Spectroscopic Analysis. Diffuse reflectance spectroscopy and Raman vibrational analysis were performed on our compounds; the data from **I** and **III** will be presented here. Diffuse reflectance spectra confirm that the compounds are electron precise phases comprising Pu(III). Figure 7 shows the two spectra in the region from 300 to 1300 nm. The compounds display optical transitions that very closely resemble those found for Pu(III) in perchloric acid, with some minor differences.³ Peaks appear in both spectra at 495, 532, 595, 630, 690, 800, 910, 940, 1060, 1135, and 1166 nm. There are distinct differences in the intensities of several peaks, most notably the peak at 495 nm. The near-IR peaks in **III** are broader and weaker than in **I**, although these intensity differences may be attributed to the sample size and preparation.

Raman spectra reveal vibrational transitions for both phases that are common among previously prepared thiophosphate compounds.^{31,32} Table 6 lists the transitions observed together with those seen in CuHgPS_4 and $\text{Ag}_4\text{P}_2\text{S}_7$, a compound that contains the corner-sharing $\text{P}_2\text{S}_7^{4-}$ polyhedra.^{31,32} Tentative assignments have been made based on those made for these other two compounds. Only a detailed vibrational analysis using isotopic substitutions will reveal the true assignments of the vibrations observed.

Conclusions

We have extended the study of solid-state actinide chemistry using molten alkali-metal thiophosphate melts to include plutonium. With the isolation of **I**, which is related to our 4f-element phase $\text{K}_3\text{La}(\text{PS}_4)_2$, and the observation that compounds **I–IV** are related to the recently reported KSmP_2S_7 , we can

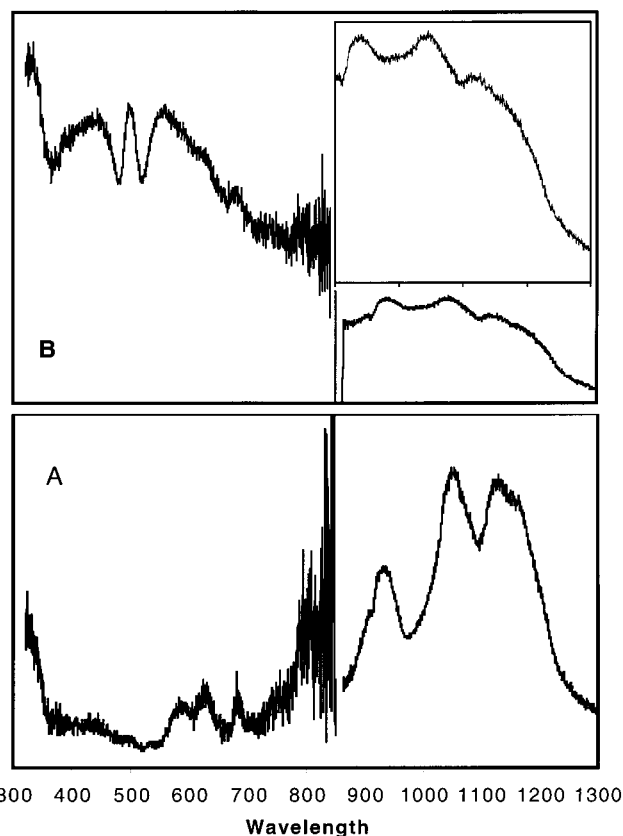


Figure 7. Diffuse reflectance spectra of (A) $\text{K}_3\text{Pu}(\text{PS}_4)_2$, **I**, and (B) RbPu_2S_7 , **III**. There is a detector change at 850 nm. The inset in (B) shows the 900–1300 nm region ($\times 3$).

Table 6. Raman Shift Data for $\text{K}_3\text{Pu}(\text{PS}_4)_2$, **I**, and RbPu_2S_7 , **III**

| $\text{K}_3\text{Pu}(\text{PS}_4)_2$, I | CuHgPS_4 , ref 31 | assign PS_4 in T_d | RbPu_2S_7 , III | $\text{Ag}_4\text{P}_2\text{S}_7$, ref 32 | assign P_2S_7 in C_{2v} |
|--|-------------------------------|----------------------------------|---|---|--|
| 213 w | | | 219 m | 203 m | ν_{20} (B_2) |
| 229 m | 236 m | ν_2 (E) | 247 m | 247 m | ν_9 (A_2) |
| 299 s | 298 s | ν_4 (T_2) | | 300 m | ν_{13} (B_2) |
| 411 s | 402 vs | ν_1 (A_1) | 410 s | 400 vs | ν_3 (A_1) |
| 440 w | | | 472 m | 477 m | ν_{17} (B_2) |
| | 509 w | ν_3 (T_2) | | | |
| | 532 m | ν_3 (T_2) | | 516 m | ν_2 (A_1) |
| | 570 m | ν_3 (T_2) | | 555 m | ν_2 (A_1) |
| | | | | 590 w | ν_1 (A_1) |
| | | | | 602 w | ν_{12} (B_1) |
| 666 w | | | 641 w | | |
| 680 w | | | | | |

conclude that the thiophosphate chemistry of plutonium is more rare-earth-like than that of the earlier actinide elements thorium and uranium. The data suggest that our hypothesis that the chemistry of plutonium quaternary chalcogenide compounds will resemble that of the rare earth chemistry has been supported by several examples. Nevertheless, an extensive study of the phase space has not revealed all the phases we and others have observed for La through Yb.^{5,12,14,15}

Finally, we have established coordination geometry preferences (bicapped trigonal prismatic or distorted square antiprismatic) for the PuS_8 polyhedra as well as bond distance parameters that are consistent with the few other known Pu(III) sulfides and oxysulfides: 2.850–3.050 \AA for a typical Pu–S bond; longer bonding interactions were also found up to 3.210 \AA , generally in the face-capping atoms of a bicapped trigonal prism

(30) Wells, A. F. *Three-dimensional Nets and Polyhedra*; John Wiley & Sons: New York, 1977.

(31) Menzel, F.; Brockner, W.; Carrillo-Cabrera, W. *Heteroat. Chem.* **1993**, *4*, 393–398.

(32) Mentzel, F.; Ohse, L.; Brockner, W. *Heteroat. Chem.* **1990**, *1*, 357–362.

of sulfurs around plutonium(III). These bond distances are also consistent with the An–S distances found in our previously reported Th(IV) and U(IV) thiophosphates.⁹ Our ongoing studies in complex plutonium and neptunium chalcogen materials will continue to elucidate some of the mysteries that surround these unusual elements.

Acknowledgment. This research was supported by the Department of Energy, Office of Basic Energy Sciences Grant DE-FG03-97ER14797 and the G. T. Seaborg Institute for Transactinium Science at Los Alamos National Laboratory. We

also thank David L. Clark for helpful discussions, Brian L. Scott for assistance with the crystallography, and Anthony J. Lupinetti and Antonio A. Maestes for assistance in the laboratory.

Supporting Information Available: Additional crystallographic details, tables of all bond distances, angles, and anisotropic thermal parameters (PDF). This information is available free of charge via the Internet at <http://pubs.acs.org>.

JA0108133